Polymer 51 (2010) 3669–3684

Contents lists available at ScienceDirect

Polymer

journal homepage: www.elsevier.com/locate/polymer

Low percolation threshold conductive device derived from a five-component polymer blend

Sepehr Ravati, Basil D. Favis*

CREPEC, Department of Chemical Engineering, École Polytechnique de Montréal, Montréal, Québec, H3C3A7, Canada

ARTICLE INFO

Article history:
Received 8 April 2010
Received in revised form
1 June 2010
Accepted 7 June 2010
Available online 12 June 2010

Keywords:
Polymer blend
Conductive
Morphology

ABSTRACT

In this work we report on the preparation of a solid, 3D, low percolation threshold conductive device prepared through the control of multiple encapsulation and multiple percolation effects in a 5 component polymer blend system through melt processing. Conductive polyaniline (PANI) is situated in the core of the 5 component continuous system comprised of high-density polyethylene (HDPE), polystyrene (PS), poly(methyl methacrylate)(PMMA) and poly(vinylidene fluoride)(PVDF). In this fashion, its percolation threshold can be reduced to below 5 vol%. The approach used here is thermodynamically controlled and is described by Harkins spreading theory. In this work the detailed morphology and continuity diagrams of binary, ternary, quaternary and finally quinary systems are progressively studied in order to systematically demonstrate the concentration regimes resulting in the formation of these novel multiple-encapsulated morphological structures. Initially, onion-type dispersed phase structures are prepared and it is shown that through the control of the composition of the inner and outer layers the morphology can be transformed to a hierarchical-self-assembled, multi-percolated structure. The influence of a copolymer on selected pairs in the encapsulated structure is also examined. The conductivity of the quinary blend system can be increased from 10^{-15} S cm^{-1} (pure HDPE) to 10^{-5} S cm^{-1} at 5 vol% PANI and up to 10^{-3} S cm^{-1} for 10 vol% PANI. These are the highest conductivity values ever reported for these PANI concentrations in melt processed systems.

1. Introduction

Over the last 30 years the polymer–polymer blending of conventional polymers has received significant attention since these materials can result in highly synergistic property sets. Although a vast number of studies have been devoted to the study of immiscible polymer blends and of the dispersed phase-matrix, fibrillar, and co-continuous morphologies, relatively few studies have focused on blends containing three or more components with complex morphologies [1–4].

Ternary A/B/C systems can exist in two possible states. One is known as complete wetting and the other is partial wetting. Complete wetting can result in B and C droplets individually dispersed in an A matrix. It can also result in the case where one B or C phase completely engulfs the other in a matrix of A. In this latter case, the minimization of interfacial free energy occurs when, for example, phase B is situated at the interface of, and completely wets, phases A and C. Phase B prevents any contact between phases A and C (Fig. 1a). In the partial wetting state, all three phases have an interface with each other (Fig. 1b). In such a case intact droplets of B, for example, can be placed at an A/C interface. Recently some very novel structures have been generated via partial wetting [5,6].

Strict thermodynamic conditions need to be met in order to have either discrete phases, encapsulated structures or partial wetting. Torza and Mason [7] and then Hobbs et al. [8] employed a modified Harkins spreading theory (Equation (1)) to predict whether the morphology of a ternary blend is dominated by complete engulfing or by partial wetting.

$$\lambda_{12} = \gamma_{23} - \gamma_{13} - \gamma_{12} \quad (1)$$

where λ is the spreading coefficient, γ represents the interfacial tension for various polymer pairs where the sub-indexes refer to each component. If one of the spreading coefficients such as λ_{12} has a positive value, a complete engulfing case occurs in which phase 1 separates phases 2 and 3 (Fig. 1a). In another case, where all spreading coefficients have negative values, the system exhibits partial wetting in which all phases have contact with each other (Fig. 1b). It has been shown that Harkins equation is, on the whole,

* Corresponding author. Tel.: +1 (514) 3404711x4527; fax: +1 (514) 3404159.
E-mail address: basil.favis@polymtl.ca (B.D. Favis).

0032-3861/$ – see front matter © 2010 Elsevier Ltd. All rights reserved.
doi:10.1016/j.polymer.2010.06.015

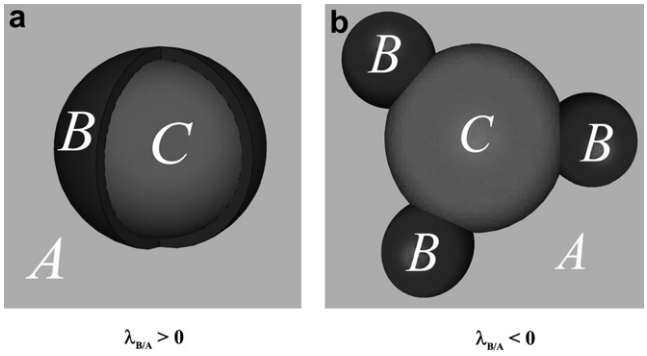

Fig. 1. Schematic representation of a) the complete engulfing case where phase B spreads between, and fully separates, phases A and C and b) the partial engulfing case all phases are in contact with each other.

a good criterion to predict the position of phases in ternary polymer blends [2,4,6,9]. As the number of phases increases to four however, it is difficult to determine the morphology by such a simple model. To date, there is no equation or model which predicts where the phases will situate in a multi-blend system comprising more than three phases.

Co-continuous morphologies represent the special case where, in an A/B system, both components are fully continuous within the blend. This type of system is referred to as a single-percolated structure. Recently [4,10,11], some papers are examining the potential of double percolated structures by locating a phase with a specific characteristic at the interface of two other continuous phases. For example, Zhang et al. [4] by employing Harkins equation and controlling the composition of phases, developed a double-percolated structure in which polystyrene was situated at the interface of high-density polyethylene and poly(methylmethacrylate). All three phases were shown to be fully continuous.

The best-known utilization of a double-percolated morphology is locating intrinsically conductive particles or polymers at the interface of binary blend of common polymers to produce a conductive polymer composite [12–14]. Classic percolation theory is usually utilized to explain the transition from discontinuous phase behavior to continuous phases. In conductive materials, this transition point is defined as the critical concentration of conductive phase required to build up a first conductive pathway and is referred to as the percolation threshold. The percolation threshold is generally defined as the onset of long-range connectivity in random systems. By employing a double percolated structure, the percolation threshold of the middle phase sharply decreases as its presence is limited only to the interface. The conductivity of a conductor-insulator blend near the percolation threshold point is calculated by the following equation:

$$\sigma = \sigma_0 (p - p_c)^t \tag{2}$$

where σ_0 is the conductivity at the percolation threshold point, σ is the conductivity of the blend, p is the concentration of the conductive material, p_c is the percolation threshold concentration, and t is a dimensionless index.

The classic percolation threshold for a random dispersion of hard-core spheres in a matrix in three dimensions is approximately 16 vol% [15]. Restricting the dispersed phase spatially, for example in interfacial tension driven structures such as a double-percolated morphology, can significantly reduce the percolation threshold of that phase. In that case the particles or polymer components can be precisely located at the interface leading to dramatic reductions in the percolation threshold value [4,16,17]. In other words, by controlling the morphology of the blend and restricting the pathways of the components, the percolation threshold deviates from the standard value of percolation threshold in a random system predicted by percolation theory. Moreover, using the same approach, controlling the morphology of the system can also influence the behavior of conductive systems. Confining the pathways of a conductive material in a multiphase system can result in high conductivities at low concentration of conductive material. The dimensionless index t in Equation (2) represents the effect of the morphology of the system on the conductivity behavior. This has already been shown to be possible for conductive systems where the conductive phase was selectively localized in the multiphase blend and consequently the concentration threshold for the onset of electrical conductivity was significantly decreased [13].

In the case of conductive fillers, both the size and shape of the particles influence the percolation threshold. Typically the percolation threshold ranges from 10 to 40% volume fraction of the conductive filler [18]. It has also been theoretically and experimentally observed that for polymer blends including a dispersed metal [19] or carbon black [20] phase, that the percolation threshold depends on the aspect ratio of the filler and it decreases when the ratio of the length to the diameter increases [21]. Gubbels et al. reported a percolation threshold as low as 3 wt% carbon black when it is localized in one phase of a binary blend consisting of 45% polyethylene and 55% polystyrene [16,17]. Then, they showed that localization of carbon black at the interface of a co-continuous PE/PS blend exhibits a sharp reduction in the percolation threshold value to 0.5 wt%. Blends consisting of conductive material prepared slightly above the percolation threshold have low conductivity. The most difficult part is preparing the conductive blend near the percolation threshold with reproducible conductive results. Sumita et al. [22] developed a criterion based on spreading coefficients to define the conditions for localization of carbon black at the interface.

After the discovery of doped polyacetylene and its metal-like behavior, research shifted from carbon black to intrinsically conductive polymer blends (ICP). By replacing the inorganic semiconductors in conventional device structures with a semiconducting polymer, the basic application of these materials has already been demonstrated [23]. They can store information and energy, and are capable of performing intelligent functions. The most amenable conductive polymer to solution processing and melt-processing [24] is polyaniline (PANI). Investigations by Macdiarmid et al. [25], which resulted in the discovery of electrical conductivity for the emeraldine salt of polyaniline, led to an explosion of interest in this fascinating polymer. The emeraldine base of PANI is soluble in a few strong acids [26]. Various dopants were utilized to induce melt-processability in PANI. The main disadvantage of all intrinsically conductive polymers including PANI is its limited melt-processability. The addition of zinc compound to doped-PANI complex is a method for tailoring the processability of sulfonic acid-doped PANI [27,28]. It has been observed that for polymer blends containing PANI, a range of conductivity between 10^{-10} S cm^{-1} to 10^{-1} S cm^{-1} (melt processing) and 10^{-10} S cm^{-1} to 10 S cm^{-1} (solution processing) can be achieved [29].

The blending of PANI with a variety of classical polymers to improve the mechanical properties of PANI and also to decrease the percolation threshold of the conductive polymers has been extensively studied. Conductive binary polymer blends can demonstrate good mechanical properties with conductivity varying from 10^{-11} S cm^{-1} (almost insulating) to 300 S cm^{-1}. It should be noted that different techniques including melt-blending, solution blending, in-situ polymerization, and dispersion mixing have different influence on PANI morphology and subsequently on properties. For instance, in the case of a PS/PANI blend, although melt-blending results in a higher PANI percolation threshold than dispersion mixing, a significant improvement in mechanical properties is achieved via the melt blending approach [30]. Most studies of polymer blends

Table 1
Material characteristics.

Material	Supplier	Commercial Code	Mw $\times 10^{-3}$ (g/mol)	$\eta^* \times 10^{-3}$ at 190 °C and 25 s^{-1}(Pa s)	Density (g/cm^3) at 20 °C	Density (g/cm^3) at 200 °C
Poly(methyl methacrylate)	Aldrich	–	12	0.04[a]	1.19	1
Polystyrene	Dow	615APR	290	1.5	1.04	0.97
High density Polyethylene	Dow	–	79	0.72	0.98	0.85
Polyaniline	Panipol	CX	–	0.11[b]	–	1.07
Polyvinylidene fluoride	Arkema	Kynar Flex	–	1.4[c]	–	1.6
PS-co-PMMA (40% Styrene)	–	–	100–150	34[d]	–	0.98

[a] Reported by Reignier et al. [2].
[b] Viscosity measured at 180 °C.
[c] Zero shear viscosity of PVDF is 902 000 Pa s at 190 °C calculated by Carreau-Yasuda model.
[d] Zero shear viscosity (Pa s).

containing PANI have been performed in solution and only a few melt-blending studies have been reported [31–34]. Polystyrene (PS) [35], Cellulose acetate [36], Polymethylmethacrylate (PMMA) [37], Polyethylene (PE), Polypropylene (PP), Polyamide (PA) [38], Polyimide (PI) [39], Polyvinyl chloride (PVC) [40], Polyurethane (PU) [41], and a wide variety of thermoplastic elastomers [42,43] have been blended with PANI using a variety of techniques other than melt-blending [30–34].

A conductivity value of 0.1 S cm^{-1} for 20 wt% of PANI is observed for PS/PANI blend prepared by in-situ polymerization [35]. Using a polymer solution blending approach, Cao et al. [44] developed a processing method for a host polymer of PMMA and polyaniline optimally doped with camphor sulfonic acid. Using this method the value of electrical conductivity could be increased to 1 S cm^{-1} for loading levels of polyaniline as low as 0.3% (vol/vol) [45]. The solution blending of PANI and its derivatives with poly(vinylidene fluoride)(PVDF) have attracted significant interest due to some of the special properties of PVDF, namely, excellent mechanical properties, chemical and weathering resistance, piezo-electric properties and good flexibility [46,47]. Fraysse et al. [48] were able to decrease the percolation threshold of PANI sharply in a PANI/PMMA solution blend to 0.5 wt% of PANI. Although the above methods using in-situ polymerization and polymer solution blending can result in very low percolation thresholds of conductive polymer, they suffer from serious disadvantages such as poor mechanical properties. In addition, clearly the environmental and health related issues associated with solvents and solvent removal are critical concerns. A melt blending approach, from this point of view, is potentially a much more robust and environmentally friendly approach.

In the case of melt-processing, Shacklette et al. [31] reported percolation thresholds in a range of 6–10 wt% for PANI dispersed in polar polymers such as polycaprolactone and poly(ethylene terphthalate glycol). Zilberman et al. [11] have reported percolation thresholds of PS/PANI and linear low-density polyethylene (LLDPE)/PANI of about 30 wt% of PANI. They reported a lower percolation value of 20 wt% PANI for the binary blend composed of copolyamide 6/6.9(CoPA)/PANI.

Levon et al. [49] were the first to suggest the concept of double percolation in a ternary polymer blend consisting of a conductive polymer. This double percolated system was comprised of a connected path within a connected path, the latter of which is conducting. Zilberman et al. [11] observed a high-quality conductive PANI network in a CoPA/LLDPE/PANI ternary blend and a poor-quality PANI network in a (PS + dioctyl phthalate (DOP))/LLDPE/PANI blend. Narkis and coworkers [30,50,51]extended and developed these previous works by blending PANI with other homopolymers via different methods mostly by using the methodology of a double percolated morphology to decrease the percolation threshold and improve mechanical properties. They showed that for several melt processed PANI/polymer blends, the conductivity results reveal a percolation threshold of approximately 20 wt%. That work also shows that, in ternary blends consisting of PANI and two immiscible polymers, the PANI is preferentially located in one of the constituting polymers. They found that PANI always prefers to locate in one phase rather than situating at the interface [11]. In all previous works performed on PANI, the percolation threshold concentration of PANI was determined based on the onset of increase in the conductivity as a function of composition. In most of those cases, the sample conductivity at the percolation threshold point is between 10^{-11} S cm^{-1} and 10^{-9} S cm^{-1}. In order to have higher conductivity values, higher concentrations of PANI are required.

This work reports on the development of onion morphology and multi-percolated morphologies in HDPE/PS/PMMA/PVDF/PANI blends in which all phases are assembled hierarchically in order. The overall objective is to lower the percolation threshold value of PANI to the lowest possible value. The required thermodynamic conditions to obtain these structures will be examined. The effect of the number of components, phase composition and the influence of an interfacial modifier on the conductivity of the blends will be examined.

2. Experimental methods

2.1. Materials

Commercial HDPE, PS, PMMA, processable PANI, and fluoropolymer (PVDF) were examined in this work. The main characteristics of the materials used in this study are represented in Table 1. Cyclohexane, acetic acid, dimethylformamide (DMF), and chromic acid were used to extract or dissolve the selected phases.

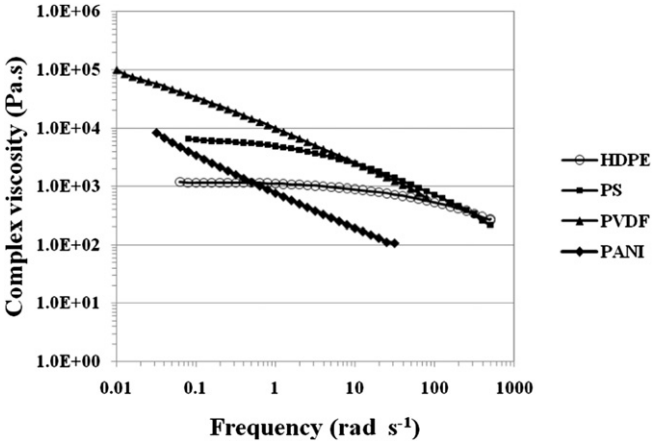

Fig. 2. Complex viscosity as a function of frequency at 190 °C for the homopolymers. The complex viscosity of PANI is at 180 °C.

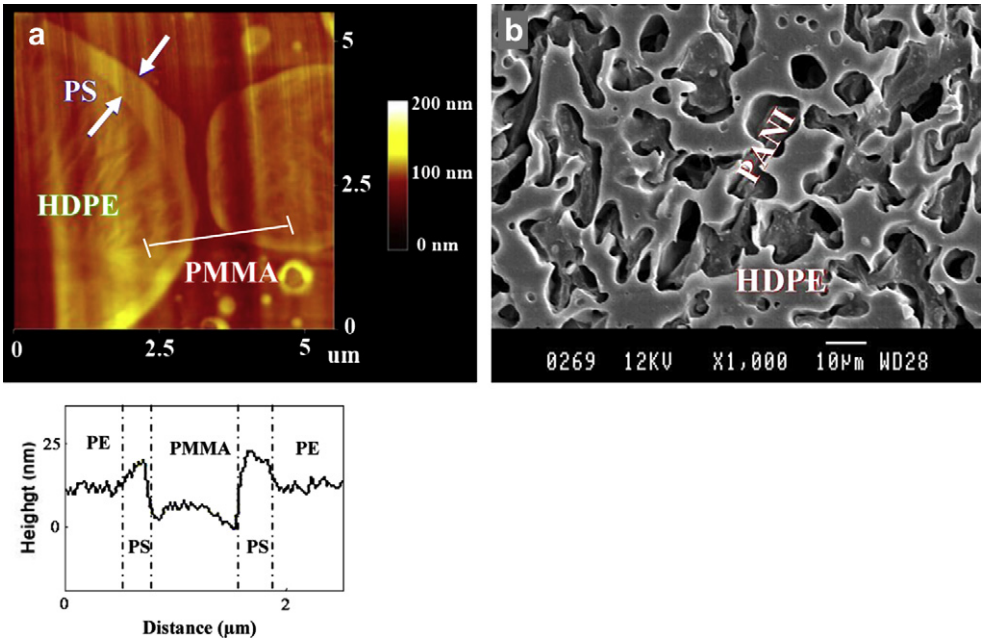

Fig. 3. a) FIB-AFM image of the composite-droplet morphology of 30/10/60 HDPE/PS/PMMA showing PS as a layer separating HDPE and PMMA. Scan size is 5.5 µm × 5.5 µm. The bar to the right of the FIB/AFM micrograph indicates the colours associated with the topographical height in nm. The white line in the image indicates the section analyzed below, and b) SEM micrograph of a 45/10/45 HDPE/PVDF/PANI blend after extraction of the PVDF phase by DMF. The voids show that PVDF was present as a layer separating HDPE and PANI.

PANI was purchased from Panipol Ltd, in the form of cylindrical compressed pellets with a composition of about 25 wt% polyaniline salt and 75 weight % of a zinc compound to modify its processability. The specific conductivity of this material is about 5 S cm^{-1}.

2.2. Rheological analysis

The rheological characterization of the neat polymers was measured using a Bohlin constant stress rheometer (CSM) in the dynamic mode. PS, PMMA, HDPE, and PVDF are known to follow the Cox–Merz equation [52], consequently, the applied frequency can be considered as the shear rate and the complex viscosity as the steady shear viscosity. Measurements were carried out at 190 °C under a nitrogen atmosphere. The complex viscosities are plotted as a function of frequency in Fig. 2. The viscosities of homopolymers at 25 s^{-1} are reported in Table 1. All polymers show shear-thinning behavior and the Carreau-Yasuda model [53] was used to determine the zero-shear viscosity of PVDF.

2.3. Sample preparation

Various blends were prepared via melt-blending under a flow of dry nitrogen in a 30 mL Brabender operating at a set temperature of 200 °C and 50 rpm. The maximum shear rate at this speed is close to 25 s^{-1}. The real temperature achieved by the end of mixing experiment was approximately 185 °C. A value of 0.7 fill factor was selected and thus after converting the volume to the mass and weighing the material, the mixing chamber was filled to 70% of its total volume. A concentration of 0.2 wt% of Irganox antioxidant supplied by CIBA was added to the mixture to reduce the thermal oxidation of the components. All the blends were mixed for 8 min. After average 2 min mixing time the torque achieves a constant plateau value. After mixing, the samples were immediately cut from the mass and quenched in a cold water bath to freeze-in the morphology.

In order to produce disk-shaped samples of 2.5 cm diameter and 1.2 mm thickness for conductivity testing, a hot press was employed. The press is heated to 200 °C and the mould is filled with blend pellets. To facilitate the de-molding of the material, two sheets of Teflon are inserted between the plaques. The total molding cycle takes 8 min under a nitrogen purge gas. A large cold press was employed after hot press to decrease the temperature sharply to avoid annealing of the sample.

2.4. Solvent extraction

A solvent extraction/gravimetric method was used to obtain quantitative data on the extent of continuity of the phases. Selective solvents were used to extract the specimens of various masses at room temperature. The volume of the components before and after

Table 2
Surface tension, polar contribution, dispersive contribution, polarity, and rate of surface tension per temperature for homopolymers.

Polymers	γ (mN/m) at 20 °C	γ (mN/m) at 200 °C	γ^p/(mN/m) at 200 °C	γ^d (mN/m) at 200 °C	Polarity, X^p	$(-d\gamma/dT)$ (mN/m K)
HDPE[a]	35.7	25.4	0	25.4	0	0.057
PS[a]	40.7	27.7	4.6	23.1	0.167	0.072
PMMA[a]	41.1	27.4	7.7	19.7	0.28	0.076
PVDF[b]	33.2	22.9	8.7	14.2	0.376	0.057
PANI[c]	55.6	40.3	24.6	15.7	0.612	0.085

[a] From Ref. [55].
[b] From Ref. [56].
[c] Measured by contact angle method.

Table 3
Theoretical and experimental interfacial tension for polymer pairs.

Theoretical data (Harmonic mean equation) γ (mN/m)				Experimental data γ (mN/m)	
PS/HDPE	4.7	PMMA/HDPE	8.4	PS/HDPE[a]	5.1
PMMA/PS	1.1	PANI/HDPE	26.9	PMMA/PS[a]	2.4
PVDF/HDPE	11.9	PVDF/PMMA	1	PMMA/HDPE[b]	8.5
PVDF/PS	3.4	PVDF/PANI	7.7		
PANI/PMMA	9.3	PANI/PS	15.1		

[a] From Ref. [2].
[b] Measured by breaking thread method.

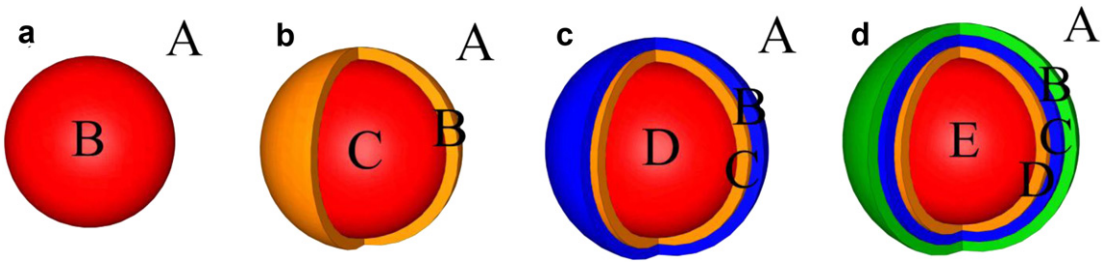

Fig. 4. Schematic illustration of various encapsulated structures, a) dispersed phase B in matrix A, b) core-shell morphology B/C in matrix A, c) quaternary onion morphology B/C/D in matrix A, and d) quinary onion morphology B/C/D/E in matrix A.

extraction is measured by weighing the sample and converting the weight to volume (Equation (3)). As a primary advantage, solvent extraction is an absolute measurement and is also a straightforward technique to detect the existence of co-continuous microstructures when the components are soluble in specific solvents.

$$\%\text{Cocontinuity} = \frac{\sum_n V_{\text{initial}} - \sum_n V_{\text{final}}}{\sum_n V_{\text{initial}}} \times 100 \quad (3)$$

Where V_{initial} and V_{final} are the volume of one component present in the sample before and after extraction calculated by weighing the sample and converting it to the volume. The degree of continuity represents the fraction of a phase that is continuous. Samples in which each phase has a degree of continuity of 1.0 are completely continuous. The reported value is the average of several samples and the average error for high continuity levels is ±5% and for low continuity levels is ±3%. Cyclohexane, acetic acid, and chromic acid were utilized as selective solvents for polystyrene, polymethyl methacrylate, and polyaniline, respectively and DMF extraction was performed to dissolve PS, PMMA, and PVDF altogether.

2.5. Characterization of phase morphology

2.5.1. Microtoming and scanning electron microscopy (SEM)

The specimens were cut and microtomed to a plane face under liquid nitrogen using a microtome (Leica-Jung RM 2065) equipped with a glass knife and a cryochamber type (LN 21). After the appropriate chemical treatment at room temperature with selective solvents (acetic acid for PMMA, cyclohexane for PS, chromic acid for PANI, and DMF for all three of PVDF, PMMA, and PS) to remove one or several of the components, the sample surface was coated with a gold/palladium alloy by plasma deposition. A JEOL JSM 840 scanning electron microscope, operated at a voltage of 10–12 keV, was used to obtain photomicrographs of the sample surface.

2.5.2. Focused ion beam (FIB), atomic force microscopy (AFM)

A FIB/AFM technique was used to examine the PE/PS/PMMA blend. After cryomicrotoming of the specimens using a glass knife to obtain perfectly flat surface, samples were coated with a gold-palladium alloy. The surface of the samples was then treated and etched using a Hitachi focused ion beam FIB-2000A operated at 30 keV. FIB uses a focused beam of gallium ions which are accelerated to energy of 5–50 keV. Using an electrostatic lens, ion beam can be focused on a very small spot, resulting in a high resolution because of the small emitting area. In this work, a 0.8 nA beam current and a dwell time at 3 μs was applied in order to remove approximately 3–4 μm of the surface. Milling was carried out parallel to the observed surface. Since each polymer component has a different interaction with the gallium beam, this approach induces topological differences and hence increases the contrast between components. The milled surface of the specimen was then examined by a scanning probe microscope with a Nanoscope IIIa controller in topological mode. The atomic force microscope (AFM) measures topography with a force probe. Silicon tips with spring constant of 40 N/m and a resonant frequency of around 300 kHz were employed.

2.6. Conductivity measurements

DC electrical measurements were performed through the vertical thickness of the substrate at ambient temperatures using a Keithley electrometer model 6517. The sample is placed between two sample holders and a DC voltage is applied using two point probe equipment. The setup works at a voltage range of 0–1000 V and an ammeter range of 0–20 mA. To standardize equal pressure for all samples, a 2.27 kg (5 lb) load was applied on the sample holders. Cylindrical specimens with a thickness of 1.2 mm and a radius of 1.25 cm were tested in dry air. Although the top and bottom surfaces of the samples are flat, two graphite sheets covered the surface of the sample in order to ensure good contact of the sample surface and electrodes. The electrical conductivity of the samples varied over a wide range from 10^{-12} S cm^{-1} to 10^{-1} S cm^{-1}. The average error in the conductivity measurements is ±0.2 orders of magnitude.

3. Results and discussions

3.1. Reducing the percolation threshold of PANI in a multi-component polymer blend

The principal objective of this work is to control the morphology of a multi-component polymer blend in order to significantly reduce the percolation threshold of the conductive PANI

Table 4
Spreading coefficients in different ternary blends and predicted order of phases in blends.

	Ternary blend and order of phases in the blend	Spreading coefficients λ (mN/m)		Ternary blend and order of phases in the blend	Spreading coefficients λ (mN/m)
1	HDPE|PS|PMMA	$\lambda_{PS/PMMA} = 2.6$ mN/m	6	HDPE|PS|PANI	$\lambda_{PS/PANI} = 7.1$ mN/m
2	HDPE|PS|PVDF	$\lambda_{PS/PVDF} = 3.8$ mN/m	7	HDPE|PVDF|PANI	$\lambda_{PVDF/PANI} = 7.3$ mN/m
3	HDPE|PMMA|PVDF	$\lambda_{PMMA/PVDF} = 2.5$ mN/m	8	PS|PMMA|PANI	$\lambda_{PMMA/PANI} = 4.7$ mN/m
4	PS|PMMA|PVDF	$\lambda_{PMMA/PVDF} = 1.3$ mN/m	9	PS|PVDF|PANI	$\lambda_{PVDF/PANI} = 4$ mN/m
5	HDPE|PMMA|PANI	$\lambda_{PMMA/PANI} = 9.2$ mN/m	10	PMMA|PVDF|PANI	$\lambda_{PVDF/PANI} = 0.6$ mN/m

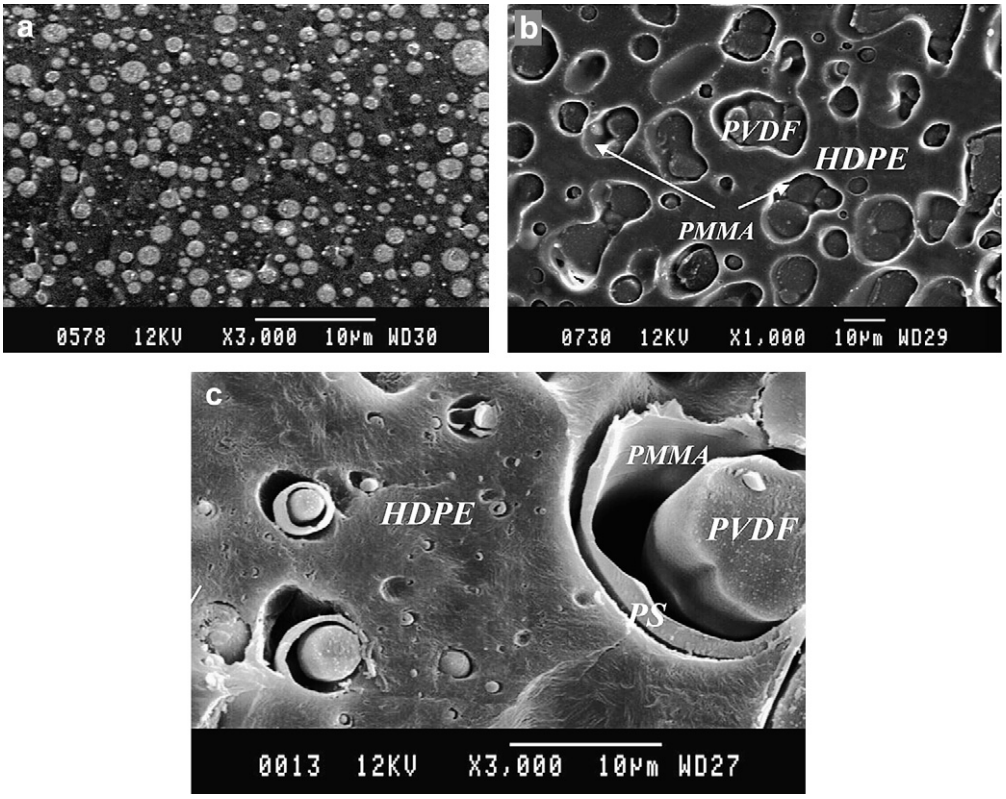

Fig. 5. SEM micrograph of a) matrix-droplet morphology of 80/20 PMMA/PS, b) PVDF core-PMMA shell morphology in an HDPE matrix for 60/20/20 HDPE/PMMA/PVDF (PMMA extracted), and c) onion morphology in an HDPE matrix for 60/13/13/13 HDPE/PS/PMMA/PVDF (PMMA extracted).

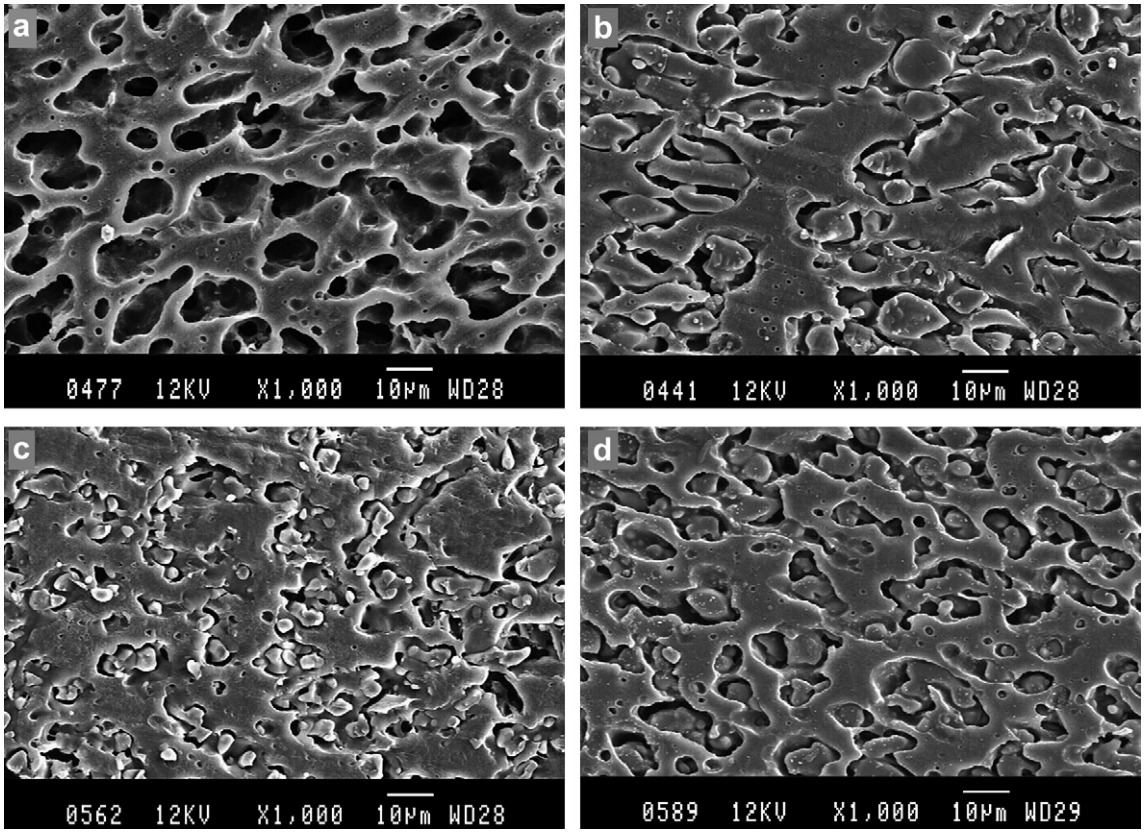

Fig. 6. SEM micrographs of 50/20/10/10/10 HDPE/PS/PMMA/PVDF/PANI after extraction of a) all phases except HDPE, b) PS by cyclohexane c) PMMA by acetic acid, and d) PS and PMMA by combining cyclohexane and acetic acid.

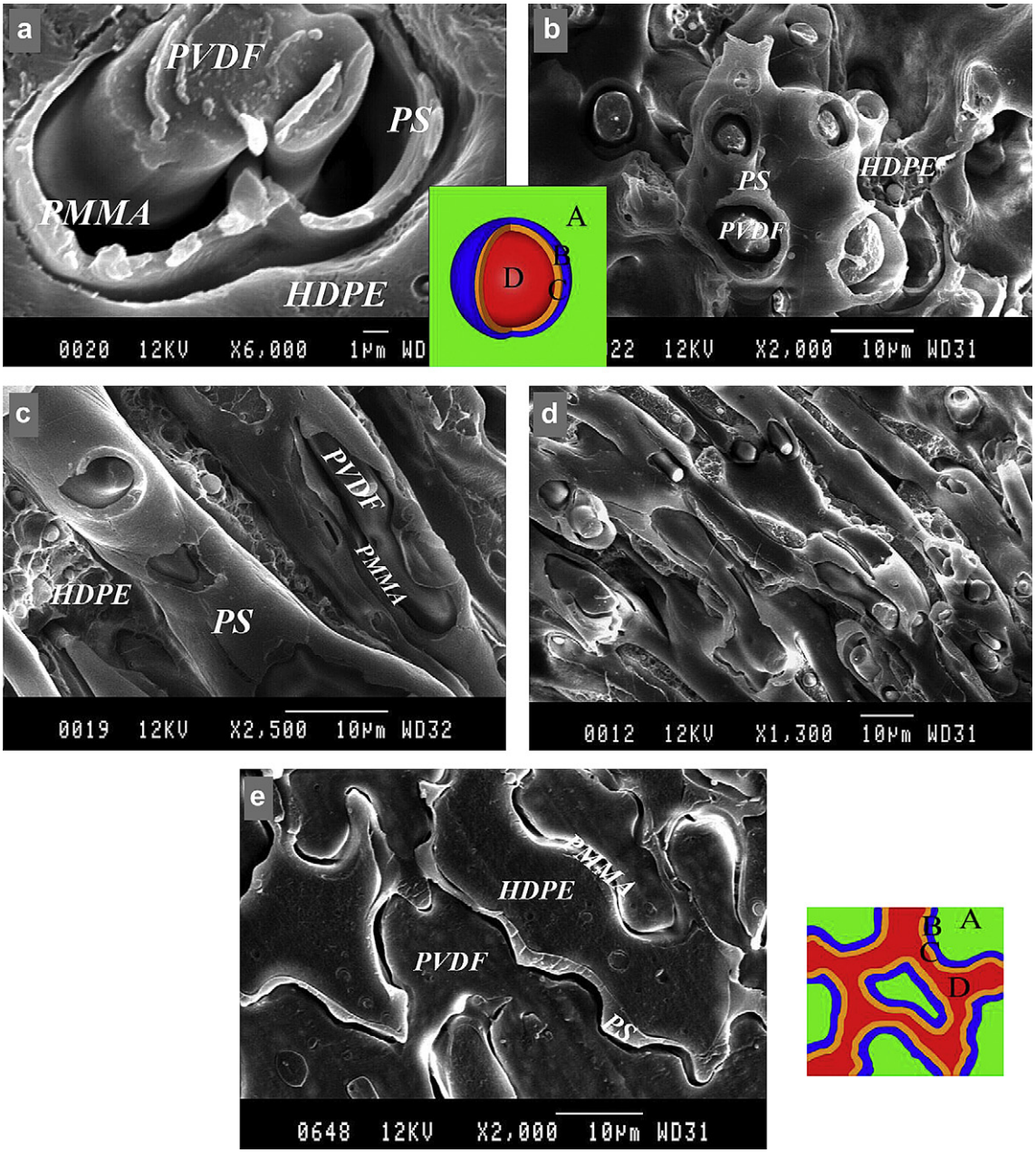

Fig. 7. SEM micrographs and schematics of HDPE/PS/PMMA/PVDF after extraction of PMMA by acetic acid for a) and b) onion morphology in an HDPE matrix for 60/13/13/13, (cryofracture), c) and d) more elongated morphology of 50/17/17/17, (cryofracture), and e) triple-percolated morphology of 30/15/15/40 (microtomed surface). The voids show that PMMA is present as a layer separating PS and PVDF.

component. The first question to be addressed is where does the PANI need to be located in the blend system?

In recent work, Zhang et al. [4] demonstrated that the percolation threshold of one component could be reduced to values as low as three percent by preparing a ternary blend and situating that phase at the interface of two other co-continuous phases. In Fig. 3a, it is shown that polystyrene situates at the interface of PE and PMMA and the ordering of the phases can be directly related to Harkins spreading theory. In Fig. 3a, the identification of the phases can be clearly seen by the topographical heights induced by FIB etching and subsequently quantified by AFM analysis in the topographical mode. Previous work showed that PMMA is less etched than HDPE which is less etched than PS [54]. The positive spreading coefficient of PS over PMMA ($\lambda_{PS/PMMA}$) with a value of 2.6 mN/m predicts the development of a thermodynamically stable PS layer between the PE and PMMA phases and is a direct result of the very high interfacial tension of PMMA and HDPE ($\gamma_{HDPE/PMMA} = 8.4$ mN/m).

Table 2 represents the surface tension and polarity of the various polymers being used in the harmonic mean equation [55] for interfacial tension. Table 3 shows a range of interfacial tension values of polymer pairs, including PANI with other polymers, estimated using the harmonic mean equation. A number of these interfacial tensions were also measured experimentally in this research group and they show a good correlation with the harmonic mean data (Table 3).

The harmonic mean equation approach is a classic approach for estimating the interfacial tension of polymer pairs and has been used widely in a number of studies [55]. It can be seen that,

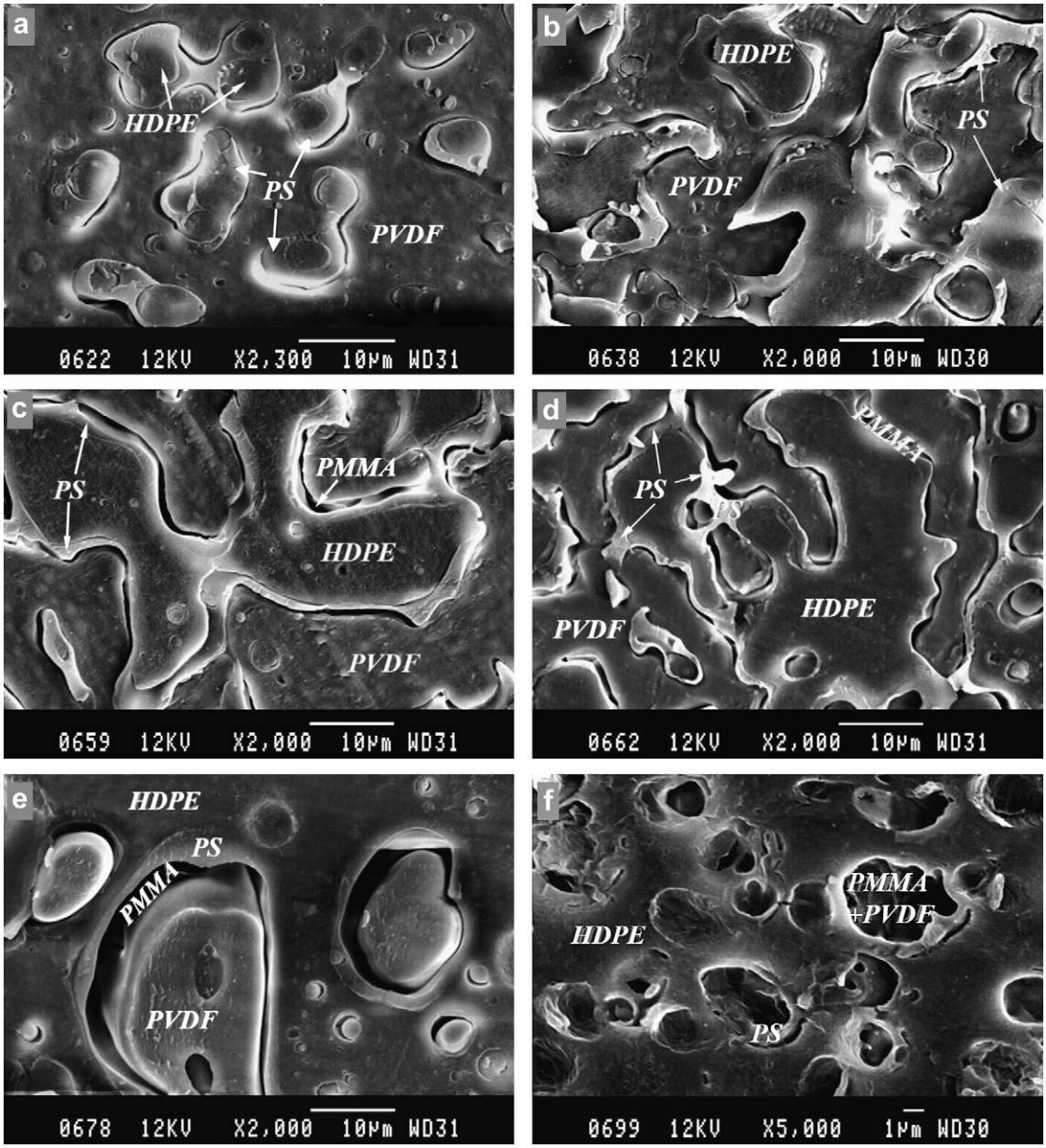

Fig. 8. SEM micrographs of various quaternary HDPE/PS/PMMA/PVDF blends after microtoming and extraction of the PMMA phase; a) 10/15/15/60, b) 20/15/15/50, c) 30/15/15/40, d) 40/15/15/30, e) 50/15/15/20 and f) 60/15/15/10.

compared to other polymer pairs, mixtures with PANI result in exceptionally high interfacial tensions. It thus follows from spreading theory that PANI will not be driven to encapsulate other polymers in a multi-component blend, rather it will tend to be encapsulated by virtually every other polymer species. For example, in a ternary HDPE/PVDF/PANI blend, a positive spreading coefficient value of 7.3 mN/m for $\lambda_{PVDF/PANI}$ predicts encapsulation of PANI by PVDF as confirmed in Fig. 3b. In that figure, the voids left by the extracted PVDF can be clearly seen to show that PVDF formed an interlayer between HDPE and PANI.

By increasing the number of components in a multi-percolated structure, the percolation threshold of all phases sharply decreases. Thus, a unique approach to achieve a low percolation threshold conductive PANI device would be to prepare a multiple percolated blend system with PANI as the innermost phase. In this work we will examine the progressive morphological development of highly continuous multi-component structures by first examining the development of multi-encapsulated ternary to quinary droplets which are referred to here as *onion* morphologies. Then, the required conditions for transformation of the onion morphology to continuous multi-percolated morphologies and the conductivity of those systems are examined.

3.2. Self-assembled onion morphology and the hierarchical ordering of phases

Typically, in the literature, a core/shell morphology is used to describe a droplet comprised of one phase encapsulated by another single phase. Here, we use the term onion morphology, schematically shown in Fig. 4, to describe a multi-phase, multi-encapsulated dispersed droplet structure. In other words, a polymeric droplet phase comprised of layers of different polymers assembled

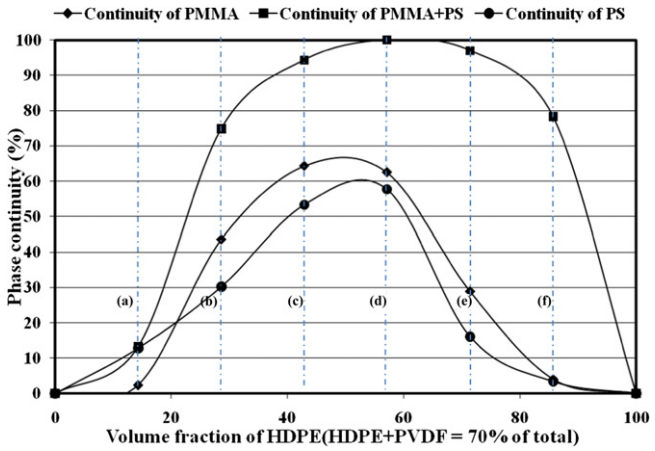

Fig. 9. Continuity level of PS, PMMA, and PS + PMMA obtained by solvent extraction/gravimetry for 6 blends comprised of HDPE/PS/PMMA/PVDF; a) 10/15/15/60, b) 20/15/15/50, c) 30/15/15/40, d) 40/15/15/30, e) 50/15/15/20 and f) 60/15/15/10.

concentrically. Fig. 4 shows schematically the progression from a matrix-droplet (Fig. 4a) to a core/shell (Fig. 4b) and finally two cases of onion morphology (Fig. 4c and d).

The thermodynamic conditions to obtain such onion structures for a given *n*-component blend is that the spreading coefficients of each of three selected components out of *n* components should satisfy the complete engulfing case in Harkins equation. At the same time, the order of phases in each selected ternary blend should be consistent with the order of the phases situated in the multi-blend. This implies that for a core/shell structure, as there are only three phases in the blend system, only one set of Harkins equation needs to be examined. In the case of a quaternary blend system with an onion structure, a combination of three out of four which is equal to four systems of Harkins equation should be evaluated. Finally in this study, ten systems of Harkins equation (equivalent to three out of five components) should be evaluated for a quinary blend system, which in the present work is comprised of HDPE, PS, PMMA, PVDF, and PANI. Both the interfacial tensions and the spreading coefficients for these ten binary pairs are shown in Tables 3 and 4, respectively.

The first four ternary blends in Table 4 indicate that in a quaternary blend comprised of an HDPE matrix with PS, PMMA, and PANI, the order of components from outer to inner should be: HDPE|PS|PMMA|PVDF. Using the data from Tables 3 and 4 it is also predicted that various other quaternary mixtures should assemble hierarchically as follows: HDPE|PS|PMMA|PANI (see spreading coefficients 1, 4, 5 and 8 in Table 4); HDPE|PMMA|PVDF|PANI (spreading coefficients 3, 5, 7 and 10); HDPE|PS|PVDF|PANI (spreading coefficients 2, 6, 7, and 9); and PS|PMMA|PVDF|PANI (spreading coefficients 4, 8, 9, and 10). Finally, from the above, the quinary blend should have the hierarchical ordering of HDPE|PS|PMMA|PVDF|PANI.

After a theoretical determination of the order of all phases, morphology experiments for the binary, ternary, and quaternary blends comprised of the previously mentioned components confirm the theoretical ordering. Some examples are shown in Fig. 5. The binary blend of 80/20 PMMA/PS with matrix-droplet morphology is shown in Fig. 5a. A ternary blend of 30/10/60 HDPE/PS/PMMA blends has already been shown in Fig. 3a and confirms the situation of PS at the interface of PE and PMMA which corresponds to the positive value of $\lambda_{PS/PMMA}$ (2.6 mN/m) (Case 1 from Table 4) as already discussed. Another ternary blend of 60/20/20 HDPE/PMMA/PVDF is shown in Fig. 5b. In that case the PMMA has been selectively extracted showing clearly a core/shell structure where PMMA is the shell and PVDF is the core. This HDPE/PMMA/PVDF ternary blend corresponds to $\lambda_{PMMA/PVDF}$ (2.5 mN/m) (Case 3 from Table 4) which predicts an encapsulation of PMMA about PVDF. The morphology observed for a quaternary blend of 50/20/10/20 HDPE/PS/PMMA/PVDF, shown in Fig. 5c, is also consistent with the theoretical ordering discussed above. Fig. 5c shows the onion-like microstructure of the quaternary blend after selective dissolution of PMMA. The selective dissolution of PMMA allows for the clear identification of the other phases. There is a core of PVDF encapsulated in a first shell of PMMA, encapsulated in second shell of PS, all of which are encapsulated by the HDPE matrix.

Theoretically, the addition of PANI as a fifth component to the quaternary blend above, creates a five-component onion droplet structure with PANI as the inner phase and HDPE as the matrix. Since it is difficult to isolate the position of PANI in a 5 component blend system, a ternary blend of HDPE/PVDF/PANI, already shown in Fig. 3b was prepared. The morphology of this blend, after selective extraction of the PVDF, clearly shows the localization of PVDF at the interface of HDPE and PANI which is a result of the very high spreading coefficient of PVDF over PANI, $\lambda_{PVDF/PANI}$ (7.3 mN/m). These data on the PE/PVDF/PANI blends as well as the discussion related to the other ternary and quaternary blend systems above would tend to confirm the ordering of phases in the quinary system as HDPE|PS|PMMA|PVDF|PANI as predicted from Harkins spreading theory.

Although detecting the position of each phase in a five-component onion structure by microscopy techniques is very difficult, the morphology of 50/20/10/10/10 HDPE/PS/PMMA/PVDF/PANI blend after selective extraction of one or several phases is represented in Fig. 6. Fig. 6a depicts the continuous structure of HDPE after extraction of all other phases. Empty spherical areas observed in the matrix of HDPE represent onion domains containing various phases. The selective extraction of PS (Fig. 6b) and PMMA (Fig. 6c) phases from the blend verifies them as two layers of an onion. Fig. 6d shows the same blend where phases PS and PMMA have been extracted together demonstrating a wider empty area, indicating the successive situation of PS and PMMA phases. The extracted area in Fig. 6d separates two major phases which are the matrix of HDPE and droplet-in-droplet of PANI-in-PVDF. All of the above confirms the hierarchical ordering of HDPE|PS|PMMA|PVDF|PANI in the quinary blend.

3.2.1. Generating highly continuous (multiple-percolated) quaternary polymer blends

In this part of the work the composition range required to achieve multiple percolation for quaternary HDPE/PS/PMMA/PVDF blends, where all phases are continuous and percolated through the system, will be determined. In such a case, not only does the typical percolation threshold of the multiphase blend decrease due to the increased number of components, but also the specific percolation threshold of each of the individual phases (middle, inner, and outer) significantly decreases.

The most critical phases in HDPE/PS/PMMA/PVDF are the first (HDPE) and last (PVDF) phases. Changing the ratio of these two phases, while maintaining the concentration of the middle phases controls the evolution of the morphology from an onion structure to a multi-percolated one. It has been shown in previous work from this laboratory [57] that composite droplets with a core/shell morphology can experience coalescence and still maintain the hierarchical order after coalescence. Fig. 7a–e, which shows quaternary HDPE/PS/PMMA/PVDF blends of concentrations of 60/13/13/13(onion morphology), 50/17/17/17, and 30/15/15/40 (multi-percolated morphology), illustrates that the hierarchical order is maintained as the morphology transits from an onion structure to more elongated structures through to a multi-

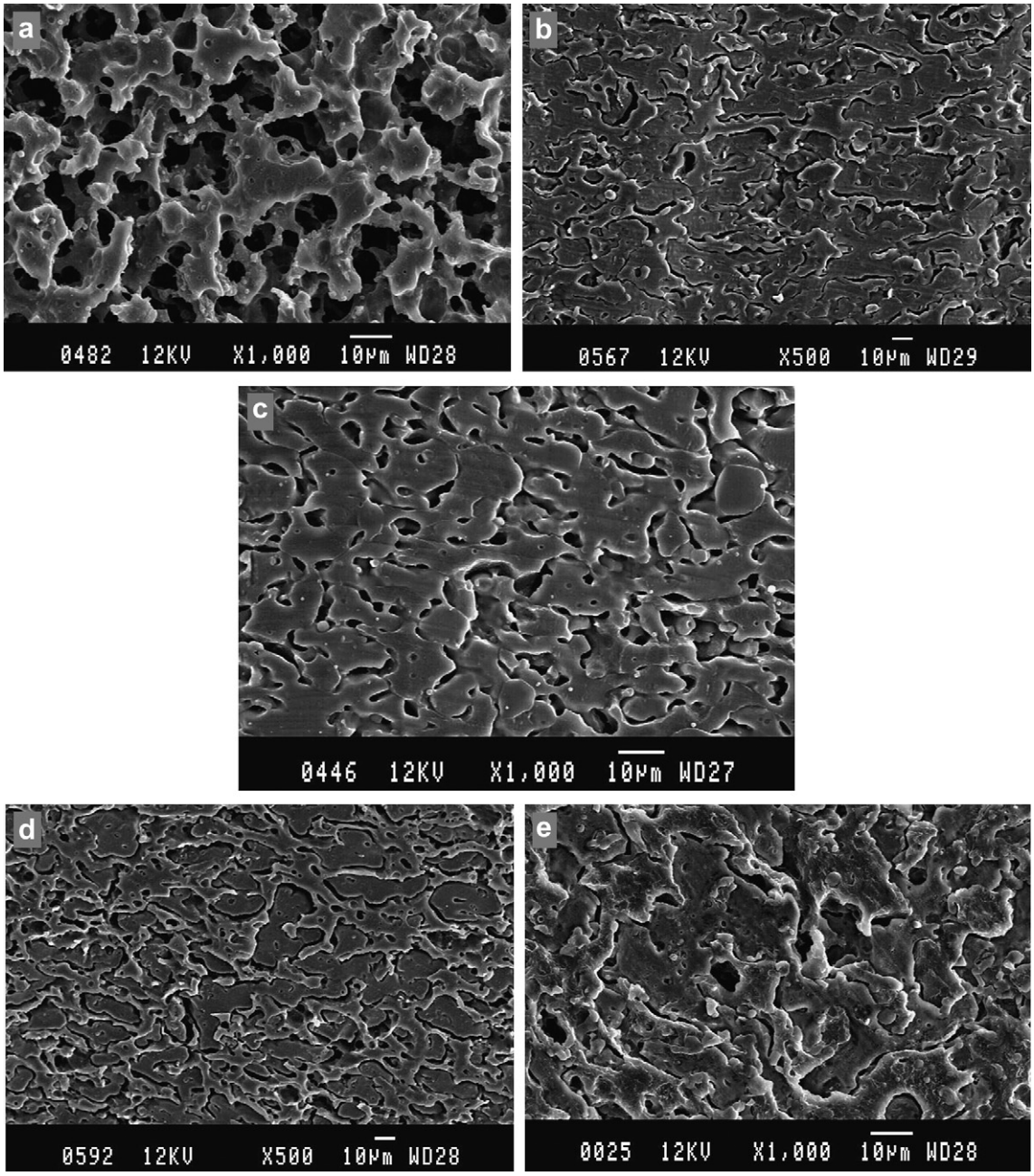

Fig. 10. SEM micrographs of the multi-percolated 30/15/15/30/10 blend comprised of HDPE/PS/PMMA/PVDF/PANI after extraction of a) all phases except HDPE, b) PMMA by acetic acid c) PS by cyclohexane, d) PS and PMMA by combining cyclohexane and acetic acid, and e) PANI by chromic acid.

percolated one. Fig. 7e shows unambiguously, after the selective extraction of the PMMA phase, that highly ordered multi-percolated morphology is obtained for 30HDPE/15PS/15PMMA/40PVDF with a hierarchical ordering of HDPE/PS/PMMA/PVDF.

Uniform layers of PS and PMMA situated in the middle of a quaternary blend of HDPE/PS/PMMA/PVDF are found at concentrations levels of 15% for each respectively. In order to determine the range of multi-percolated regions in the quaternary HDPE/PS/PMMA/PVDF blend, the composition ratio of HDPE and PVDF is varied from 10/15/15/60 HDPE/PS/PMMA/PVDF to 60/15/15/10 HDPE/PS/PMMA/PVDF while the composition of PS and PMMA is maintained at 15% (Fig. 8).

Fig. 8 illustrates the morphologies obtained and in all cases PMMA has been extracted by acetic acid to distinguish it from HDPE, PS, and PVDF in the blend. Hence, PMMA can be recognized as void areas separating the continuous parts of the PS layer attached to HDPE and continuous PVDF. When the composition of HDPE is as low as 10% and 20%, droplets of HDPE encapsulated by the PS phase are detected, and both are encapsulated by PMMA in a matrix of PVDF (Fig. 8a and b). The opposite behavior is encountered when the PVDF phase has concentrations as low as 10% and 20%, demonstrating droplets of PVDF encapsulated by PMMA phase where both are encapsulated by PS within an HDPE matrix (Fig. 8e and f). A comparison of 10/15/15/60 HDPE/PS/PMMA/PVDF (Fig. 8a) and 60/15/15/10 HDPE/PS/PMMA/PVDF (Fig. 8f) reveals that, although the order of phases does not change, the onion morphology is reversed depending on the concentration of the inner phase or outer phase.

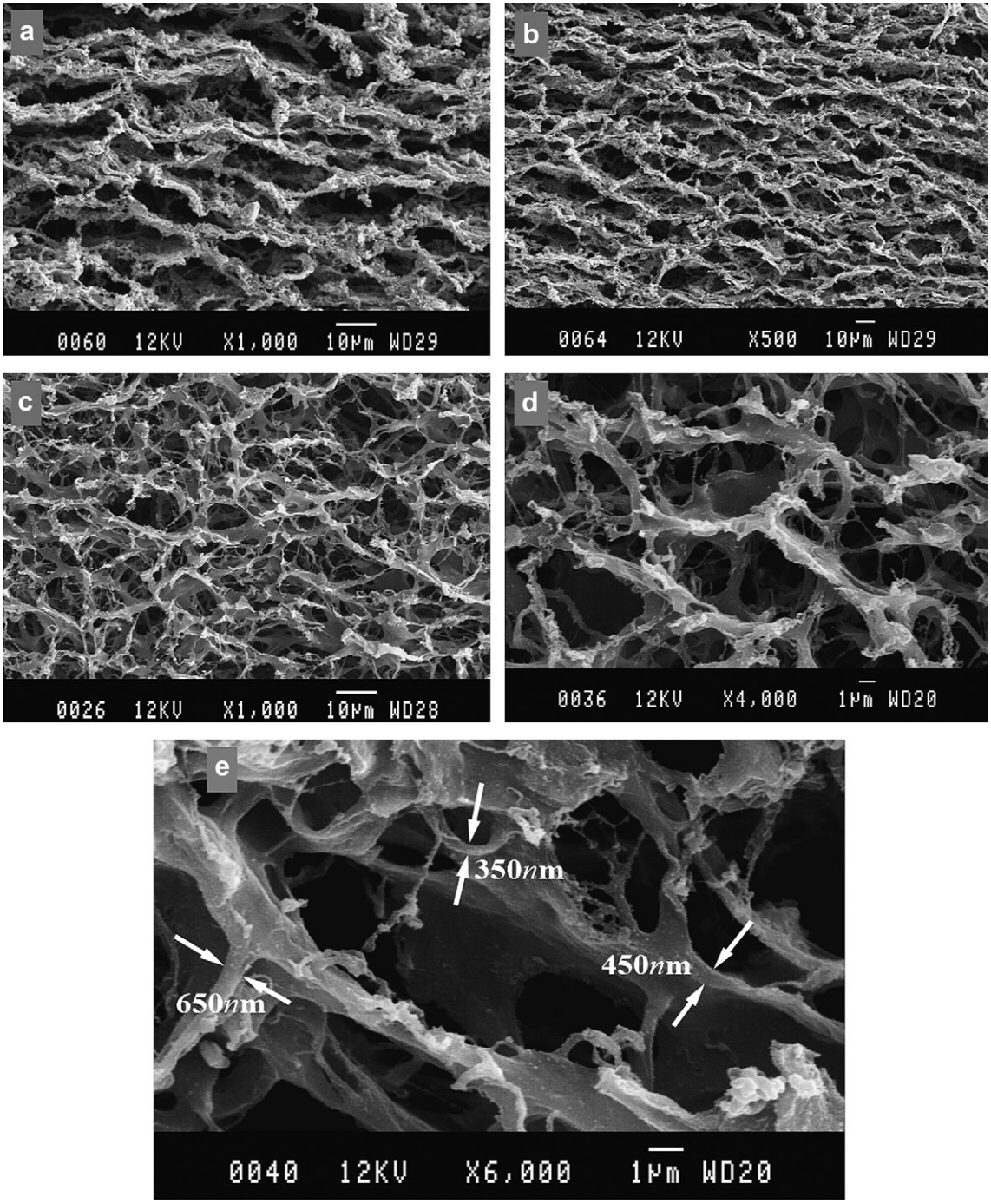

Fig. 11. SEM micrographs of a), b) continuous PANI network of quaternary 25/25/25/25 PS/PMMA/PVDF/PANI blend after extraction of all phases by DMF followed by a freeze drying process, and c–e) continuous PANI network derived from a 15/20/15/25/25 PS/PS-co-PMMA/PMMA/PVDF/PANI blend after extraction of all phases by DMF followed by freeze drying process. The thicknesses of the PANI network walls are shown in e).

As the concentration of HDPE or PVDF further increases and reaches 30%, droplets of those phases coalesce and continuous structures of the respective phase form. Blends of 30/15/15/40 HDPE/PS/PMMA/PVDF and 40/15/15/30 HDPE/PS/PMMA/PVDF show two continuous phases of HDPE and PVDF while continuous PS and PMMA phases are situated at the interface (Fig. 8c and d).

In order to find the precise region of multi-percolation quantitatively, solvent extraction followed by a gravimetric measurement was used to obtain the percentage continuity of each phase as a function of volume fraction of HDPE in the quaternary blend of HDPE/PS/PMMA/PVDF (Fig. 9). Note that in Fig. 9 the concentrations of both PS and PMMA are held at 15%, while the combined concentration of HDPE plus PVDF is always held at 70%. In Fig. 9, the *x*-axis refers to the % concentration of HDPE in HDPE plus PVDF. Thus 100% HDPE refers to the 70HDPE/15PS/15PMMA blend while 50% HDPE refers to the 35HDPE/15PS/15PMMA/35PVDF blend.

Selective extraction associated with gravimetric measurements was carried out to obtain the continuity levels of PS, PMMA, and PS + PMMA in order to determine the concentrations where the phases are continuous. The continuity of HDPE and PVDF were estimated based on SEM photomicrographs at various compositions. Gravimetric results exhibit a low level of continuity (ranging from 5

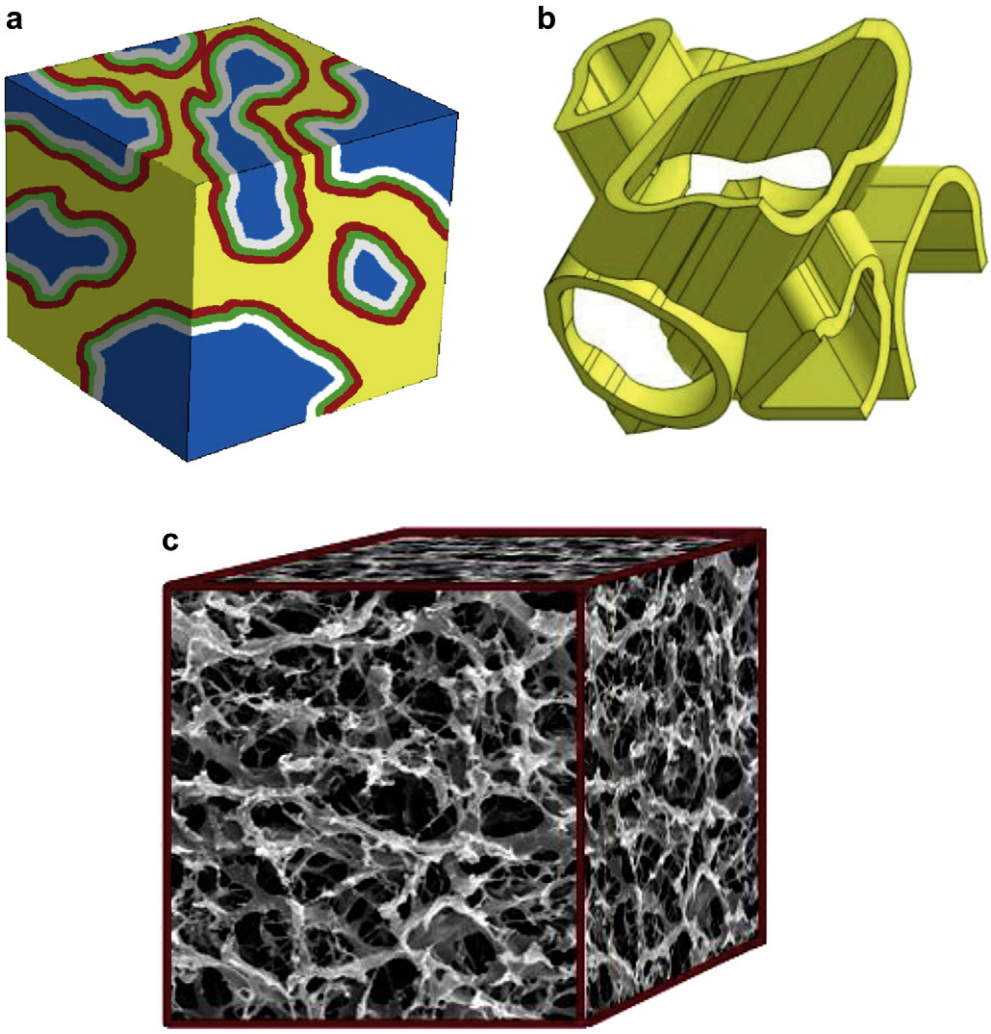

Fig. 12. a) Schematic representation of quinary multi-percolated morphology, the yellow phase is PANI, the blue phase is HDPE, and all other phases are located between them, b) schematic of a PANI network obtained after removal of all phases except PANI, and c) a 3D image constructed from 2D SEM images of the interconnected PANI network in the quinary 15/20/15/25/25 PS/PS-co-PMMA/PMMA/PVDF/PANI blend after extraction of all other phases.

to 15%) for all phases in a 10/15/15/60 HDPE/PS/PMMA/PVDF onion morphology. Increasing the concentration of HDPE to 20 parts in the blend with PVDF at 50 (28.6% HDPE on the *x*-axis) yields a hierarchical-layered morphology with an HDPE core where the continuity of PS and PMMA reaches levels of 30% and 43%, respectively. Further increasing the HDPE concentration results in a maximum continuity of all phases for blends of 30/15/15/40 HDPE/PS/PMMA/PVDF and 40/15/15/30 HDPE/PS/PMMA/PVDF (Fig. 9). If the concentration of HDPE is increased further, an inverse behavior is observed where PVDF becomes the core and HDPE becomes the matrix. In this case, for the blend containing 50HDPE/15PS/15PMMA/20PVDF, the continuity of middle phases including PS and PMMA becomes 15% and 30%, respectively. Fig. 9 shows that when the concentration of HDPE is increased up to 60 parts in the blend, the continuity of PS and PMMA becomes less than five percent.

3.2.2. Generating highly continuous quinary polymer blends

In this part of the work, the addition of a fifth component to the highly continuous quaternary blends ranging from 30/15/15/40 to 40/15/15/30 HDPE/PS/PMMA/PVDF, selected from the previous section, is examined.

Ten percent PANI is added to a quaternary blend of HDPE/PS/PMMA/PVDF within the region of multi-percolation resulting in the formation of a five-component blend of 30/15/15/30/10 HDPE/PS/PMMA/PVDF/PANI (Fig. 10). Fig. 10a shows the continuous HDPE phase after the removal of all other phases. The selective extraction of PMMA and PS reveals a perfectly homogeneous continuous network for those phases in the blend (Fig. 10b and c). The extraction of both PS and PMMA phases together separates the multi-blend into two inter-diffused continuous structures where one of them is a continuous HDPE phase and the other is a continuous PANI and PVDF phase (Fig. 10d). It also illustrates that continuous networks of PS and PMMA are adjacent to each other. In Fig. 10e, the network of PANI which has been extracted by chromic acid is clearly detected.

In order to unambiguously illustrate that PANI forms a network morphology, blends of 25/25/25/25 PS/PMMA/PVDF/PANI and 15/20/15/25/25 PS/PS-co-PMMA/PMMA/PVDF/PANI are prepared. The influence of the addition of a PS-co-PMMA copolymer on the segregation of phases is discussed in a following section in detail. After the extraction of all phases except PANI and followed by a freeze-drying process, a network of PANI with very thin walls remains, as represented in Fig. 11. Freeze-drying is carried out to prevent of shrinkage of the PANI network. This Figure clearly confirms that in a triple-percolated structure with PANI as the inner phase, PANI will spread.

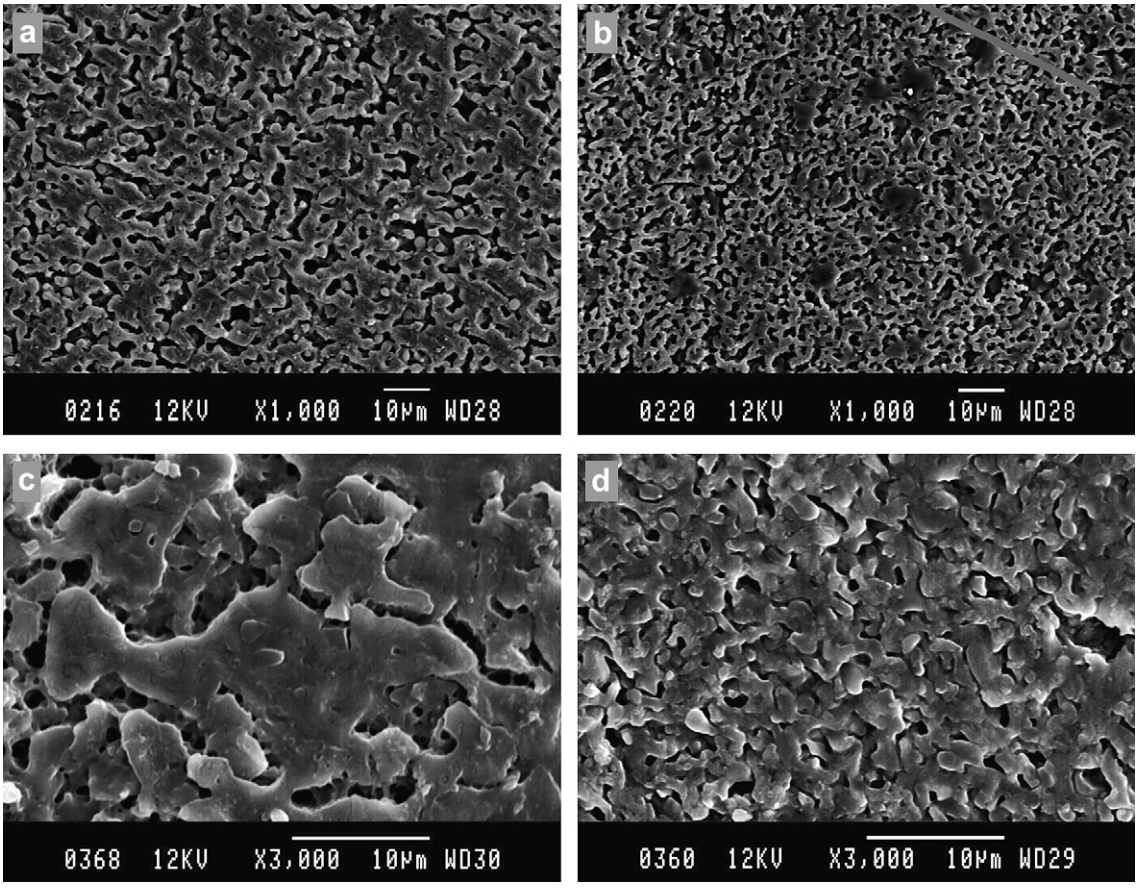

Fig. 13. SEM micrograph of a) 30/30/30/10 PS/PMMA/PVDF/PANI blend after extraction of PS and PMMA, b) 20/20/20/30/10 PS/PS-co-PMMA/PMMA/PVDF/PANI after extraction of PS and PMMA, c) 30/30/30/10 PS/PMMA/PVDF/PANI blend after extraction of PANI by chromic acid, and d) 20/20/20/30/10 PS/PS-co-PMMA/PMMA/PVDF/PANI after extraction of PANI by chromic acid.

As shown in Fig. 11e, the PANI network in a multi-percolated structure has branches with very thin walls. The range of thicknesses of the wall in this structure range from a few hundred nanometers to 700 nm. Another important point that should be taken into account is the actual content of pure PANI in the blends. The PANI used in this work is melt-processable and contains 25 wt% pure PANI and 75 wt% zinc compound. This indicates that the real volume of pure PANI present in the blends is less than reported volume fraction in these blends.

A schematic representation for such a 5-component multi-percolated structure is shown in Fig. 12a. The yellow phase represents PANI which, after removal of all other phases by selective solvents, demonstrates an interconnected network as schematically shown in Fig. 12b. Fig. 12c illustrates the 15/20/15/25/25 PS/PS-co-PMMA/PMMA/PVDF/PANI blend after extraction of all phases except PANI, clearly indicating that a complete PANI network is attained.

3.2.3. The effect of diblock copolymer on the morphology and conductivity of multiple-percolated blend systems

The addition of a PS-co-PMMA copolymer to a PS/PMMA/PVDF/PANI multi-percolated structure results in a decrease of the size of the PS and PMMA phases. Such a decrease in the size of two adjacent phases results in corresponding smaller phase sizes for the other phases involved in the multi-encapsulated structure. This can be used as an additional parameter to control morphology and conductivity.

Fig. 13 depicts two multi-percolated quaternary blends, one without modifier (30/30/30/10 PS/PMMA/PVDF/PANI) and the other with modifier (20/20/20/30/10 PS/PS-co-PMMA/PMMA/PVDF/PANI). In both cases, the composition of all the phases is identical. Fig. 13a and b compares samples with and without a copolymer, respectively, after extraction of both PS and PMMA phases using cyclohexane and acetic acid, respectively. The addition of PS-co-PMMA to the multi-percolated PS/PMMA/PVDF/PANI blend clearly reduces the sizes of all the phases.

Fig. 13c and d examines the effect of added copolymer on the phase size of PANI alone where PANI is removed using chromic acid. These micrographs show that the PANI phase size is significantly smaller after addition of PS-co-PMMA. Thus, the addition of a copolymer specific to two adjacent phases in a multi-encapsulated system results in a reduction of all phase sizes in the encapsulated system.

Fig. 11 shows the effect of copolymer more clearly on the PANI network structure after removal of all other components followed by a freeze drying step. Two blends are considered, one without copolymer, 25/25/25/25 PS/PMMA/PVDF/PANI (Fig. 11a and b), and one containing copolymer, 15/20/15/25/25 PS/PS-co-PMMA/PMMA/PVDF/PANI (Fig. 11c, d, and e). The micrographs demonstrate that, in the presence of copolymer, the PANI network is finer and more uniform with homogeneous branches distributed throughout the sample.

One question that should be addressed is whether the addition of a PS-co-PMMA interfacial modifier would be expected theoretically to affect the hierarchical order in these blend systems. Table 3 shows a very low value of interfacial tension of $\gamma_{PS/PMMA} = 1.1$ mN/m. If after addition of copolymer, $\gamma_{PS/PMMA}$ decreases to the lowest possible value close to zero, all ternary blends comprised of both PS and PMMA in the blend still show positive spreading coefficient values.

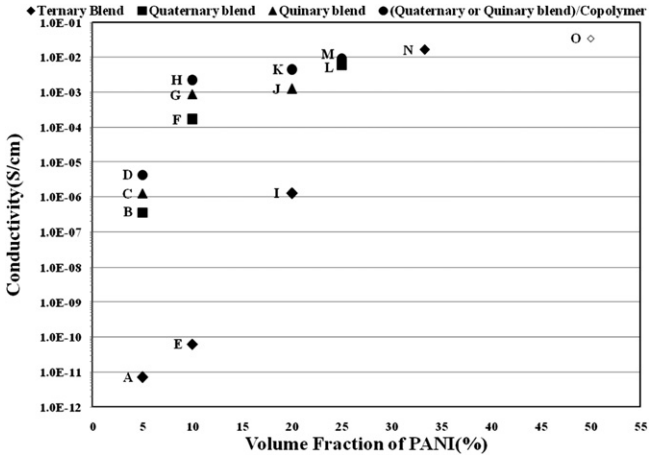

Fig. 14. Conductivity of multi-percolated blends of ternary, quaternary, quinary, as well as interfacially modified quaternary and quinary systems as a function of the volume fraction of PANI. Note that point O is a co-continuous binary blend of PS and PANI.

These results imply that the positive values of $\lambda_{PS/PMMA}$ in HDPE|PS|PMMA, $\lambda_{PMMA/PVDF}$ in PS|PMMA|PVDF, and $\lambda_{PMMA/PANI}$ in PS|PMMA|PANI result in three complete engulfing cases with the same order of phases as before the addition of copolymer.

3.2.4. The effect of the number of components of multi-percolated structures on conductivity

In this section the effect of the number of the components in multi-percolated structures on the conductivity, where PANI phase situated as the innermost phase, is investigated as a function of volume fraction of PANI (Fig. 14).

The percolation threshold for a conductive material is the concentration at which the first connected pathway of conductive polymer forms in the blend. Conductivity data thus provides a tool as powerful as solvent gravimetry to determine percolation thresholds for a conductive substance. At the concentration at which the first connected pathway of conductive polymer in the blend forms, both conductivity and continuity values sharply increase resulting in the percolation threshold. Hence, conductivity percolation threshold corresponds to continuity percolation threshold of sample. In an onion morphology with the PANI phase located at the core of a dispersed phase with low connectivity, the conductivity would be expected to be low. Fig. 14 shows samples with multi-percolated structures constituting various numbers of components. The concentration of each sample is represented in Table 5.

In Fig. 14, samples A, B, C, and D represent ternary, quaternary, five-component, and six-component polymer blends all containing five percent PANI. In all samples, the composition of all phases, other than PANI, have been selected to be in the multi-percolated region (Table 5). Sample (A) is a ternary blend of 50/45/5 PS/PMMA/PANI in which PMMA is at the interface. Due to the low amount of PANI (5 vol %) in this sample, droplets of PANI are encapsulated by the PMMA phase. The very low conductivity value of almost 10^{-11} S cm^{-1} indicates that no connected conductive pathway forms in this sample. In order to spread the PANI at least four components in the multi-percolated structure are required. In sample (B), five percent of PANI is present in a quaternary blend with a composition of 35/15/45/5 HDPE/PS/PVDF/PANI. In this blend, due to the geometrical restrictions imposed on PANI, a continuous PANI phase forms a network and the percolation threshold of PANI is achieved as seen by the conductivity value of 3.5×10^{-7} S cm^{-1}. Although the percolation threshold is defined as a transition state and occurs at different conductivity values, typically its value is between 10^{-11} S cm^{-1} and 10^{-9} S cm^{-1}. The relatively high conductivity value of 3.5×10^{-7} S cm^{-1} for sample (B) shows that percolation threshold has in fact been reached at a significantly lower concentration than 5% PANI.

Sample (C) is a quinary blend containing 5% PANI comprised of HDPE/PS/PMMA/PVDF/PANI. This system attains an even higher conductivity value of 1.2×10^{-6} S cm^{-1} thus corresponding to a lower percolation threshold due to the further geometrical restrictions imposed by the additional phase.

Sample (D) represents a blend with five components and a di-block copolymer of adjacent PS and PMMA phases in the blend. Since the PS and PMMA phases are located beside each other, the addition of their copolymer to a blend results in the size of the PS and PMMA phases being decreased (compare Fig. 13a and b). This reduction of size in the PS and PMMA phases carries over to other phases including PANI. The highest conductivity value for blend containing 5% PANI is obtained for sample (D) with a value of 4.2×10^{-6} S cm^{-1}.

The 5% percolation threshold value for PANI reported above is the lowest ever obtained in a melt processed multi-component system. Moreover, as discussed earlier, since the PANI sample used here is a mixture of 25% PANI and 75% zinc compound, the actual concentration of pure PANI at this percolation threshold value is less than 5%.

Points (E), (F), and (G) represent ternary, quaternary, and five-component blends, each of which contains 10% PANI. Point (H) is a quaternary blend containing a copolymer of PS and PMMA. Although the extent of PANI is ten percent in these cases and higher conductivity values are obtained for blends compared to samples containing 5%, a similar behavior in increasing the conductivity value with multi-percolated samples is observed. Higher concentration of PANI in the samples containing 10% PANI results in more connected pathways of PANI in the sample yielding a higher conductivity range from 6.2×10^{-11} S cm^{-1} for ternary to 2.2×10^{-3} S cm^{-1} for the quaternary blend plus copolymer.

Ternary, five-component, and six-component samples denoted as (I), (J), and (K), respectively, having 20% PANI are blended. Sample (I) shows a conductive value of 1.3×10^{-6} S cm^{-1} for the ternary blend indicating that although the PANI is encapsulated by the middle phase (PMMA), the concentration of PANI is high enough (20 vol%) to create a random network inside the PMMA. This implies that, at a high concentration of PANI, the effect of the morphology of the system on the conductivity is less important. At those higher concentrations, random connected pathways form in the system for all morphologies. But morphology is still effective whereas samples (J) and (K) comprising of more components represent higher conductivity values of 1.2×10^{-3} S cm^{-1} and

Table 5
Number of components and compositions of samples shown in Fig. 14.

Sample	Number of components	PANI	PS	PVDF	PMMA	HDPE	PS-co-PMMA
A	3	5	50	–	45	–	–
B	4	5	15	45	–	35	–
C	5	5	20	35	20	20	–
D	6	5	16	20	15	35	9
E	3	10	45	–	45	–	–
F	4	10	30	30	30	–	–
G	5	10	20	20	20	30	–
H	5	10	20	30	20	–	20
I	3	20	40	–	40	–	–
J	5	20	20	20	20	20	–
K	6	20	15	20	12	20	13
L	4	25	25	25	25	–	–
M	5	25	15	25	15	–	20
N	3	33.3	–	33.3	–	33.3	–
O	2	50	50	–	–	–	–

4.5×10^{-3} S cm^{-1}. Samples L and M in Fig. 14 with 25% PANI demonstrate that 25% of PANI in the sample is sufficient to completely diminish the effect of morphology on conductivity and random networks of PANI form everywhere in the sample. Even at higher concentrations of PANI no significant increase in conductivity for the blend is observed as random pathways saturate the sample. Since the PANI concentration and morphology of the phases in these samples have no effect on the conductivity, even ternary (sample N) and binary (sample O) blends show the maximum conductivity and plateau behavior.

4. Conclusions

We have used polyaniline as a conductive polymer to prepare a solid, 3D, low percolation threshold conductive device through the control of multiple encapsulation and multiple percolation effects in a 5 component HDPE/PS/PMMA/PVDF/PANI polymer blend system through melt processing. The percolation threshold in the multi-component polymer blend is shown to be sensitive to the morphological continuity of the various encapsulated phase networks. PANI is situated in the core of the multiple network system due to its high surface tension and polarity and, in this way its percolation threshold can be reduced to less than 5%. The detailed morphology and continuity diagrams of binary, ternary, quaternary and finally quinary systems are progressively studied in order to systematically demonstrate the concentration regimes resulting in the formation of these novel multiple-encapsulated morphological structures. First, an onion-type morphology of HDPE/PS/PMMA/PVDF is prepared which is comprised of an HDPE matrix with a multiple-component polymeric droplet phase consisting of a PS shell, a PMMA middle layer and PVDF in the core. The order of phases in this concentrically organized onion morphology is thermodynamically controlled and is described by Harkins spreading theory. Through the control of the composition of the inner (HDPE) and outer (PVDF) layers in the onion structure, the morphology can be transformed to a highly elongated onion morphology and subsequently to a multi-percolated structure in which all HDPE, PS, PMMA, and PVDF phases are continuous and percolated throughout the system. It is shown that the addition of PANI results in a 5-component multi-encapsulated, multi-percolated blend with the PANI situated in the core of the system. The addition of an interfacial modifier for the PS and PMMA components results in the diminished phase sizes of those particular components which, due to the encapsulated nature of the morphology, has the effect of reducing the phase size for all other phases as well. The conductivity is measured for a wide range of the above systems as a function of the number of phases and as a function of the PANI concentration. It is shown that increasing the number of components in the blend with a multi-percolated structure from ternary to quaternary to quinary and finally to an interfacially modified quinary blend results in a several orders of magnitude increase in the conductivity of the system. In this way, the percolation threshold of the PANI can be reduced to below 5 vol %. The conductivity of the quinary blend system, for example, can be increased from 10^{-15} S cm^{-1} (pure HDPE) to 10^{-5} S cm^{-1} at 5% PANI and up to 10^{-3} S cm^{-1} for 10% PANI. These are the highest conductivity values ever reported for these PANI concentrations in melt processed systems.

Acknowledgements

The authors express appreciation to the Natural Sciences and Engineering Research Council of Canada for supporting this work. They also thank F. Normandin from the Institut des matériaux industriels for his assistance with the conductivity measurements of the samples.

References

[1] Moussaif N, Jérôme R. Polymer 1999;40:3919.
[2] Reignier J, Favis BD. Macromolecules 2000;33:6998.
[3] Reignier J, Favis BD. AIChE Journal 2003;49:1014.
[4] Zhang J, Ravati S, Virgilio N, Favis BD. Macromolecules 2007;40:8817.
[5] Virgilio N, Marc-Aurele C, Favis BD. Macromolecules 2009;42:3405.
[6] Virgilio N, Desjardins P, L'Esperance G, Favis BD. Macromolecules 2009;42:7518.
[7] Torza S, Mason SG. Journal of Colloid and Interface Science 1970;33:67.
[8] Hobbs SY, Dekkers MEJ, Watkins VH. Polymer 1988;29:1598.
[9] Reignier J, Favis BD. Polymer 2003;44:5061.
[10] Zilberman M, Siegmann A, Narkis M. first ed., SAMPE: Anaheim, CA, USA; 1998, vol. 43, p. 528.
[11] Zilberman M, Siegmann A, Narkis M. Journal of Macromolecular Science – Physics 2000;B39:333.
[12] Pud A, Ogurtsov N, Korzhenko A, Shapoval G. Progress in Polymer Science (Oxford) 2003;28:1701.
[13] Anand J, Palaniappan S, Sathyanarayana DN. Progress in Polymer Science (Oxford) 1998;23:993.
[14] Bhattacharya A, De A. Journal of Macromolecular Science – Reviews in Macromolecular Chemistry and Physics 1999;C39:17.
[15] Scher H, Zallen R. The Journal of Chemical Physics 1970;53:3759.
[16] Gubbels F, Blacher S, Vanlathem E, Jerome R, Deltour R, Brouers F, Teyssie P. Macromolecules 1995;28:1559.
[17] Gubbels F, Jerome R, Teyssie P, Vanlathem E, Deltour R, Calderone A, Parente V, Bredas JL. Macromolecules 1994;27:1972.
[18] Jagur-Grodzinski J. Polymers for Advanced Technologies 2002;13:615.
[19] Bridge B, Tee H. International Journal of Electronics 1990;69:785.
[20] Carmona F. Physica A: Statistical and Theoretical Physics 1989;157:461.
[21] Munson-McGee SH. Physical Review B (Condensed Matter) 1991;43:3331.
[22] Sumita M, Sakata K, Asai S, Miyasaka K, Nakagawa H. Polymer Bulletin (Berlin) 1991;25:265.
[23] Burroughes JH, Jones CA, Friend RH. Nature 1988;335:137.
[24] Paul RK, Vijayanathan V, Pillai CKS. Synthetic Metals 1999;104:189.
[25] Macdiarmid AG, Jin-Chih C, Halpern M, Wu-Song H, Shao-Lin M, Somasiri LD, Wanqun W, Yaniger SI. In: Proceedings of the International Conference on the Physics and Chemistry of Low-Dimensional Synthetic Metals (ICSM 84), 17–22 June 1984; 1–4 ed. UK; 1985, vol. 121, p. 173.
[26] Andreatta A, Cao Y, Chiang JC, Heeger AJ, Smith P. Synthetic Metals 1988;26:383.
[27] Ruokolainen J, Eerikainen H, Torkkeli M, Serimaa R, Jussila M, Ikkala O. Macromolecules 2000;33:9272.
[28] Hartikainen J, Lahtinen M, Torkkeli M, Serimaa R, Valkonen J, Rissanen K, Ikkala O. Macromolecules 2001;34:7789.
[29] http://www.azom.com/details.asp?ArticleID=1197; 2000. Panipol.
[30] Segal E, Haba Y, Narkis M, Siegmann A. Journal of Polymer Science, Part B: Polymer Physics 2001;39:611.
[31] Shacklette LW, Han CC, Luly MH. Synthetic Metals 1993;57:3532.
[32] Ikkala OT, Laakso J, Väkiparta K, Virtanen E, Ruohonen H, Järvinen H, Taka T, Passiniemi P, Österholm JE, Cao Y, Andreatta A, Smith P, Heeger AJ. Synthetic Metals 1995;69:97.
[33] Narkis M, Zilberman M, Siegmann A. Polymers for Advanced Technologies 1997;8:525.
[34] Zilberman M, Titelman GI, Siegmann A, Haba Y, Narkis M, Alperstein D. Journal of Applied Polymer Science 1997;66:243.
[35] Woo Jin B, Won Ho J, Yun Heum P. Synthetic Metals 2003;132:239.
[36] Planes J, Wolter A, Cheguettine Y, Pron A, Genoud F, Nechtschein M. Physical Review B (Condensed Matter) 1998;58:7774.
[37] Morgan H, Foot PJS, Brooks NW. Journal of Materials Science 2001;36:5369.
[38] Qinghua Z, Xianhong W, Yanhou G, Dajun C, Xiabin J. Journal of Polymer Science, Part B (Polymer Physics) 2002;40:2531.
[39] Moon Gyu H, Seung Soon I. Polymer 2001;42:7449.
[40] Chipara MI, Munteanu I, Notingher P, Chipara MD, Reyes Romero J, Negreanu B, et al. Vasteras, Sweden: IEEE; 1998. p. 372.
[41] Rodrigues PC, Akcelrud L. Polymer 2003;44:6891.
[42] Dong-Uk C, Kitae S, Young Chul K, Yun Heum P, Jun Young L. Gordon & Breach: Kyoto, Japan; 2001, vol. 370, p. 399.
[43] Ong CH, Goh SH, Chan HSO. Polymer Bulletin (Berlin) 1997;39:627.
[44] Cao Y, Smith P, Heeger AJ. Synthetic Metals 1992;48:91.
[45] Yang CY, Cao Y, Smith P, Heeger AJ. Polymer Preprints, Division of Polymer Chemistry, American Chemical Society 1993;34:790.
[46] Privalko VP, Ponomarenko SM, Privalko EG, Lobkov SV, Rekhteta NA, Pud AA, Bandurenko AS, Shapoval GS. Journal of Macromolecular Science – Physics 2005;B44:749.
[47] Bliznyuk VN, Baig A, Singamaneni S, Pud AA, Fatyeyeva KY, Shapoval GS. Polymer 2005;46:11728.
[48] Fraysse J, Planes J, Dufresne A. Taylor and Francis Inc.: Poznan; 2000, vol. 354, p. 511.
[49] Levon K, Margolina A, Patashinsky AZ. Macromolecules 1993;26:4061.

[50] Haba Y, Segal E, Narkis M, Titelman GI, Siegmann A. Synthetic Metals 2000;110:189.
[51] Narkis M, Haba Y, Segal E, Zilberman M, Titelman GI, Siegmann A. Polymers for Advanced Technologies 2000;11:665.
[52] Cox WP, Merz EH. Journal of Polymer Science 1958;28:619.
[53] Yasuda K, Armstrong R, Cohen R. Rheologica Acta 1981;20:163.
[54] Virgilio N, Favis BD, Pepin M-F, Desjardins P, L'Esperance G. Macromolecules 2005;38:2368.
[55] Wu S. Polymer interface and adhesion. New York: Marcel Dekker Inc.; 1982.
[56] Baradie B, Shoichet MS. Macromolecules 2003;36:2343.
[57] Reignier J, Favis BD, Heuzey M-C. Polymer 2003;44:49.